HEFAT2012
9th International Conference on Heat Transfer, Fluid Mechanics and Thermodynamics
16 – 18 July 2012
Malta

INVESTIGATION ON OBLIQUE SHOCK WAVES OCCURRED IN THE SUPERSONIC CARBON DIOXIDE TWO-PHASE FLOW

Yosuke Kawamura* and Masafumi Nakagawa
*Author for correspondence
Department of Mechanical Engineering,
Toyohashi University of Technology,
1-1 Hibarigaoka, Tempakucho, Toyohashi City, Aichi, 441-8580,
Japan,
E-mail: kawamura@nak.me.tut.ac.jp

ABSTRACT

In the refrigeration systems using the two-phase flow ejector, it is important to understand expansion waves and shock waves which are generated at the outlet of the nozzle. The theoretical oblique shock wave relations are derived for extreme conditions. Numerical analysis of the oblique two-phase flow is also presented. Two types of two dimensional convergent-divergent nozzles with and without the inclined wall are used to measure pressure profiles along the nozzles wall. The two-phase flow in the divergent section of the nozzle obviously exhibits the supersonic decompression behavior. Numerical results can represent the experimental results with fairly good precision, but the reflections of the oblique shock wave cannot be predicted. The diameter of the droplet in two-phase flow in the nozzle is guessed by this experiment to be the order of 5 [μm] and momentum frozen phenomenon occurs in this situation. The experimental oblique shock wave has the particular character of the two-phase flow, which is never seen in single phase flow explained by gas dynamics. The observation of the present study reveals the intrinsic feature that appears only in the supersonic two-phase flow.

INTRODUCTION

The compressible two-phase flow is applied to many fields, such as geothermal power plants and refrigeration cycles. As the sound speed of the two-phase flow is low [1] compare with that of the single phase, the two-phase flow can be easily accelerated to the supersonic state and there appear shock waves. We have been studying on the supersonic two-phase flow in the ejector [2] which can improve the efficiency of the carbon dioxide refrigeration system by converting the exhausted expansion energy into the useful compression energy.

The carbon dioxide is the most hopeful refrigerant because of the low global warming. While the Global Warming Potential of the R-134a is 1500, that of the carbon dioxide is 1 from the definition. The oblique shock waves occur in the supersonic two-phase flow at the outlet of the nozzle in the ejector and the two-phase flow fields in the mixing section are affected by those waves. The one of the most important functions of the two-phase flow ejector is to compress the sucked refrigerant vapour from the evaporator and to assist the compressor. The recovered pressure depends largely on the kinetic energy of the two-phase flow at the mixing section.

We have been developing the ejector in the refrigeration cycle [3] and fundamentally researching on the characteristic of two-dimensional expansion waves [4][5] and oblique shock waves [6] in order to clarify the character of waves which occur in high speed two-phase flow.

The object of the present study is to elucidate the behaviour of the oblique shock waves of the carbon dioxide two-phase flow from experiments and analyses.

NOMENCLATURE

a	[m/s]	Sound velocity
C_p	[J/kgK]	Specific heat at constant pressure
d	[m]	Diameter of droplet
e	[J/kg]	Specific internal energy
h	[J/kg]	Specific enthalpy
h_T	[W/m^{2}K]	Heat transfer coefficient
L	[m]	Characteristic length
M	[-]	Mach number
$\dot{m}$	[kg/s]	Evaporation speed
p	[MPa]	Pressure
p_{21}	[-]	The ratio of pressure of the back to front
q	[J/m^{2}s]	Heat flux
s	[J/kgK]	Specific entropy
T	[K]	Temperature

v	[m/s]	Two-dimensional velocity
w	[m/s]	Velocity in z direction
x	[-]	Quality
z	[mm]	Coordinates along the flow direction

Special character

α	[-]	Void fraction
θ	[deg.]	Deflection angle
μ	[kg/m s]	Dynamic viscosity
ρ	[kg/m^3]	Density
τ_T	[sec]	Heat relaxation time
τ_V	[sec]	Momentum relaxation time
ϕ	[deg]	Shock wave angle

Subscripts

eq	Equilibrium condition
fr	frozen condition
g	Gas phase
l	Liquid phase
n	Vertical direction of oblique shock waves
t	Tangential direction of oblique shock waves
in	Inlet of nozzle
out	Outlet of nozzle
th	Throat of nozzle
1	Front side of the normal shock wave
2	Back side of the normal shock wave

BASIC EQUATION OF TWO-PHASE FLOW IN OBLIQUE SHOCK WAVE

The phenomena in the interphase transfer must be formalized to solve the two-phase flow in the oblique shock wave. The mass, momentum and heat transport phenomena are very important in the compressible two-phase flow.

The continuity equation of the gas and liquid phases can be expressed as:

$$\frac{\partial}{\partial t}(\alpha\rho_g)+\frac{\partial}{\partial x_j}(\alpha\rho_g v_{gj})=\dot{m}\,, \tag{1}$$

$$\frac{\partial}{\partial t}\{(1-\alpha)\rho_l\}+\frac{\partial}{\partial x_j}\{(1-\alpha)\rho_l v_{lj}\}=-\dot{m}\,. \tag{2}$$

The momentum equations of gas and liquid phases can also be expressed as:

$$\begin{aligned}&\frac{\partial}{\partial t}(\alpha\rho_g v_{gi})+\frac{\partial}{\partial x_j}(\alpha\rho_g v_{gj}v_{gi})\\&\quad=\dot{m}v_{ki}-\alpha\frac{\partial p}{\partial x_i}-(1-\alpha)\rho_l\frac{v_{gi}-v_{li}}{\tau_V}\,,\end{aligned} \tag{3}$$

$$\begin{aligned}&\frac{\partial}{\partial t}\{(1-\alpha)\rho_l v_{li}\}+\frac{\partial}{\partial x_j}\{(1-\alpha)\rho_l v_{lj}v_{li}\}\\&\quad=-\dot{m}v_{li}-(1-\alpha)\frac{\partial p}{\partial x_i}+(1-\alpha)\rho_l\frac{v_{gi}-v_{li}}{\tau_V}\,.\end{aligned} \tag{4}$$

The first term of the right-hand side of these equations expresses the amount of momentum exchange caused by the mass transfer between droplet and gas phases. The velocity v_{ki} can also be expressed as:

$$v_{ki}=\begin{cases}v_{li} & \dot{m}\geq 0\\ v_{gi} & otherwise\end{cases}.$$

τ_V denotes the momentum relaxation time and can be expressed as:

$$\tau_V=\frac{\rho_l d^2}{18\mu_g}\,. \tag{5}$$

The total energy conservation equations can be expressed as follows:

$$\begin{aligned}&\frac{\partial}{\partial t}\left\{\alpha\rho_g\left(e_g+\frac{v_{gj}^2}{2}\right)+(1-\alpha)\rho_l\left(e_l+\frac{v_{lj}^2}{2}\right)\right\}\\&+\frac{\partial}{\partial x_j}\left\{\alpha\rho_g v_{gj}\left(h_g+\frac{v_{gj}^2}{2}\right)+(1-\alpha)\rho_l v_{lj}\left(h_l+\frac{v_{lj}^2}{2}\right)\right\}=0\,,\end{aligned} \tag{6}$$

where e is the specific internal energy and h is the specific enthalpy.

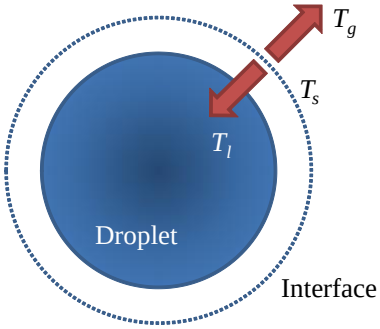

Figure 1 Model of interface heat transport

The thermal relaxation phenomenon can be described by the heat transfer equation around a sphere as shown in Figure 1 and can be written as a function of temperature difference between interface and each phase as follows:

$$q_g=h_{Tg}(T_s-T_g),\quad q_l=h_{Tl}(T_s-T_l)\,,$$

where q are the heat fluxes from the interface to each phase, and h_T for each phase expresses the corresponding heat transfer coefficients. These heat transfer equations can be rewritten in terms of entropy s. C_{pg} and C_{pl} are the specific heats of gas and liquid phases, respectively.

$$T_g\frac{D_g s_g}{D_g t}=C_{pg}\frac{1-\alpha}{\alpha}\frac{T_s-T_g}{\tau_{Tg}}\,, \tag{7}$$

$$T_l\frac{D_l s_l}{D_l t}=C_{pl}\frac{T_s-T_l}{\tau_{Tl}}\,, \tag{8}$$

where τ_{Ti} denotes the thermal relaxation times of gas and liquid phases and can also be expressed as:

$$\tau_{Tg}=\frac{\rho_g C_{pg} d}{6h_{Tg}}\,,\quad \tau_{Tl}=\frac{\rho_l C_{pl} d}{6h_{Tl}}\,. \tag{9}$$

The interface between gas and liquid is assumed to be in the saturated condition in this analysis. Therefore, the interface temperature T_s shown in Figure 1 can be calculated from pressure p of the saturation condition. This means that mass transfer is controlled by heat transport. The thermodynamic properties of CO_2 were obtained from the software REFPROP v.8 by NIST.

THEORITICAL ANALYSIS OF OBLIQUE SHOCK WAVE AT EXTREAM CONDITIONS

As described above, there are two important transport phenomena in two-phase flow, which are momentum and heat transport. Mass transfer is also essential, but in usual case, rate of mass transfer is controlled by heat transport. It is worthwhile to derive the theoretical relationship of oblique shock waves at extreme conditions. Because the relations which determine the transfer speeds are not needed for those case, and theoretical solution can be easily derived. We call equilibrium condition when the transfer speed is very high and frozen condition when it is vanishing small.

First, we derive the jump equations of normal shock waves of two-phase flow in four extreme conditions.

Momentum and Thermal Equilibrium Condition

The velocities and temperatures of each phase became equal to each other in momentum and thermal equilibrium condition. If the variables at front of normal shock wave are denoted by suffix 1, and back by 2, the mass, momentum and energy conservation relations are

Equation of continuity:

$$\{\alpha_1\rho_{g1}+(1-\alpha_1)\rho_{l1}\}w_{n1}=\{\alpha_2\rho_{g2}+(1-\alpha_2)\rho_{l2}\}w_{n2}\,. \quad (10)$$

Equation of momentum conservation:

$$\{\alpha_1\rho_{g1}+(1-\alpha_1)\rho_{l1}\}w_{n1}^2+p_1 = \{\alpha_2\rho_{g2}+(1-\alpha_2)\rho_{l2}\}w_{n2}^2+p_2\,. \quad (11)$$

Equation of energy conservation:

$$\alpha_1\rho_{g1}w_{n1}\left(\frac{w_{n1}^2}{2}+h_{g1}\right)+(1-\alpha_1)\rho_{l1}w_{n1}\left(\frac{w_{n1}^2}{2}+h_{l1}\right) = \alpha_2\rho_{g2}w_{n2}\left(\frac{w_{n2}^2}{2}+h_{g2}\right)+(1-\alpha_2)\rho_{l2}w_{n2}\left(\frac{w_{n2}^2}{2}+h_{l2}\right). \quad (12)$$

As variables at the front of shock wave are known, the unknown variables are α_2, ρ_{g2}, ρ_{l2}, w_{n2}, p_2, h_{g2} and h_{l2}. But, ρ_{g2}, ρ_{l2}, h_{g2} and h_{l2} can be calculated from the corresponding pressure at the two-phase thermal equilibrium saturation condition. Then three unknown variables α_2, w_{n2} and p_2 can be obtained from the three equations (10), (11) and (12).

Momentum Equilibrium and Thermal Frozen Condition

For the thermal frozen case, in which very little heat is transferred between phases, thermodynamics variables are function of two parameters, such as pressure and entropy. Then following two adiabatic equations must be added to above three equations (10), (11) and (12).

$$s_{g1}=s_{g2}\,,\quad s_{l1}=s_{l2}\,. \quad (13)$$

ρ_{g2}, ρ_{l2}, h_{g2} and h_{l2} can be estimated by pressure p_2 and entropy s_2 of each phase from the thermodynamic property table. Finally, five unknown variables α_2, w_{n2}, p_2, s_{g2} and s_{l2} are solved from five equations (10), (11), (12) and (13).

Momentum Frozen and thermal Equilibrium Condition

If the force acting on each other phase is so small that it can be negated in this analysis, each phase can flow independently. The momentum equations are needed for gas and liquid phase.

Equation of continuity:

$$\alpha_1\rho_{g1}w_{gn1}+(1-\alpha_1)\rho_{l1}w_{ln1} = \alpha_2\rho_{g2}w_{gn2}+(1-\alpha_2)\rho_{l2}w_{ln2}\,. \quad (14)$$

Equation of total momentum conservation:

$$\alpha_1\rho_{g1}w_{gn1}^2+(1-\alpha_1)\rho_{l1}w_{ln1}^2+p_1 = \alpha_2\rho_{g2}w_{gn2}^2+(1-\alpha_2)\rho_{l2}w_{ln2}^2+p_2\,. \quad (15)$$

Equation of droplet momentum conservation:

$$\frac{1}{2}w_{ln2}^2-\frac{1}{2}w_{ln1}^2+\int_1^2\frac{1}{\rho_l}\frac{dp}{dT}dT=0\,. \quad (16)$$

Equation of energy conservation:

$$\alpha_1\rho_{g1}w_{gn1}\left(\frac{w_{gn1}^2}{2}+h_{g1}\right)+(1-\alpha_1)\rho_{l1}w_{ln1}\left(\frac{w_{ln1}^2}{2}+h_{l1}\right) = \alpha_2\rho_{g2}w_{gn2}\left(\frac{w_{gn2}^2}{2}+h_{g2}\right)+(1-\alpha_2)\rho_{l2}w_{ln2}\left(\frac{w_{ln2}^2}{2}+h_{l2}\right). \quad (17)$$

As ρ_{g2}, ρ_{l2}, h_{g2} and h_{l2} can be estimated by the pressure p_2 form thermal equilibrium condition, four unknown variables α_2, w_{gn2}, w_{ln2} and p_2 are obtain from four equations (14), (15), (16) and (17).

Momentum and Thermal Frozen Condition

For the case in which all transport phenomena assume to be negligible, mass, momentum and energy equations are hold for each phase.

Equation of continuity:

$$\alpha_1\rho_{g1}w_{n1}=\alpha_2\rho_{g2}w_{n2}\,, \quad (18)$$

$$(1-\alpha_1)\rho_{l1}w_{n1}=(1-\alpha_2)\rho_{l2}w_{n2}\,. \quad (19)$$

Equation of momentum conservation:

$$\alpha_1\rho_{g1}w_{n1}^2+p_1=\alpha_2\rho_{g2}w_{n2}^2+p_2\,, \quad (20)$$

$$(1-\alpha_1)\rho_{l1}w_{n1}^2+p_1=(1-\alpha_2)\rho_{l2}w_{n2}^2+p_2\,. \quad (21)$$

Equation of energy conservation:

$$\alpha_1\rho_{g1}w_{n1}\left(\frac{w_{n1}^2}{2}+h_{g1}\right)=\alpha_2\rho_{g2}w_{n2}\left(\frac{w_{n2}^2}{2}+h_{g2}\right), \quad (22)$$

$$(1-\alpha_1)\rho_{l1}w_{n1}\left(\frac{w_{n1}^2}{2}+h_{l1}\right)=(1-\alpha_2)\rho_{l2}w_{n2}\left(\frac{w_{n2}^2}{2}+h_{l2}\right). \quad (23)$$

h_{g2} and h_{l2} can be estimated by pressure p_2 and density ρ_2 of each phase. Six unknown variables α_2, w_{gn2}, w_{ln2}, ρ_{g2}, ρ_{l2} and p_2 are obtained from six equations (18)-(23).

Next, the oblique shock wave relations are calculated from the normal shock wave relations. As the tangential velocity is not changed ($w_{t1}= w_{t2}$) through the oblique shock wave shown in Figure 2, the following equation is obtained from the figure.

$$\frac{\tan(\phi-\theta)}{\tan\phi}=\frac{w_{n2}}{w_{n1}} \quad i.e. \quad \theta=\phi-\tan^{-1}\left(\frac{w_{n2}}{w_{n1}}\tan\phi\right), \quad (24)$$

where θ is the deflection angle of the wall. Therefore, the shock wave angle ϕ can be calculated from equation (24) with the deflection angle θ and normal velocity ratio w_{n2}/w_{n1}. The normal velocity ratio is the same as that of normal shock waves. Provided that the deflection angle is given, the shock wave angle is determined by the normal shock wave relations.

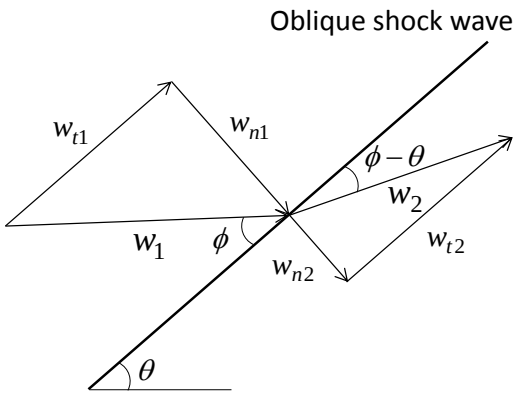

Figure 2 Velocity vector diagram at oblique shock wave

The lines for four extreme conditions plotted in Figure 3 are the oblique shock wave relations between the shock wave angle and the front Mach number. The front conditions of the oblique shock wave are set to those of the experiment which will be detailed latter. T_1=-52[ºC] and x_1=0.41.

NUMERICAL ANALYSIS

Numerical analysis is also carried out. In this study, the flow region shown in Figure 4 was used to calculate the characteristic of oblique shock waves of two-phase flow in semi-infinite field. The declined rectangle region is built by the deflection angle θ. The two-phase mixture flows from the left and upper boundaries and goes out of the domain through the right hand side boundary. Slip condition of gas phase is used for the wall boundary at the bottom. The liquid phase was assumed to go out from the domain when it reaches the wall. Actually, as the volume of droplets which adhere on the wall is negligibly small, this assumption for the liquid phase can be justified. The inlet condition was assumed to be in equilibrium condition, and the gas inlet velocity was approximated to be equal to that of liquid. The thermal boundary conditions for the wall and outlet section were set to adiabatic.

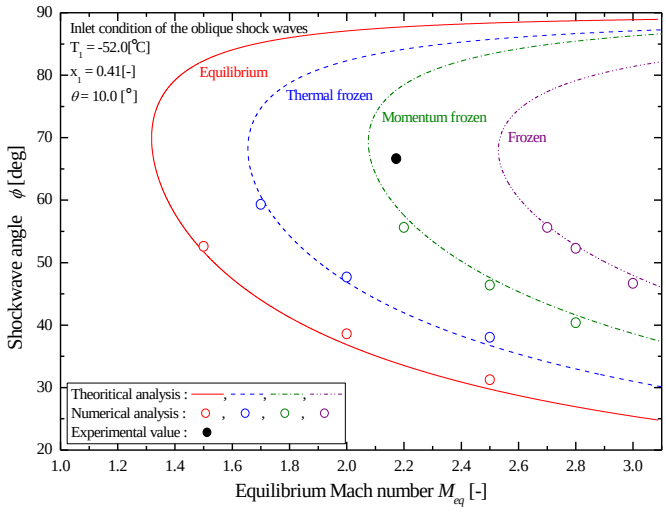

Figure 3 Shock wave angles versus front Mach number for extreme conditions

CIP-method is adopted for this study to solve the governing equations. The CIP-method has third-order resolution scheme. As equations (1)-(4) and (6)-(8) have only first derivatives respected to the time, those can be transformed into advection equations for the CIP-method.

The number of calculation grids along the flow and transverse direction were 70 and 100, respectively. The non-steady state calculation was initially carried out. The steady state solution is obtained when sum of all pressure change from two successive steps was less than 10^{-5}.

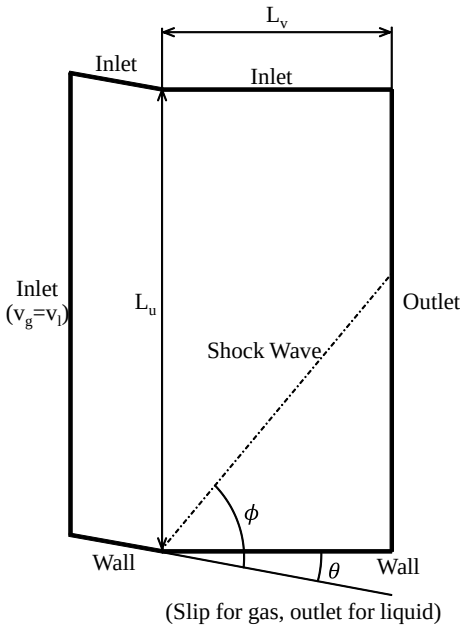

Figure 4 Region of Analysis

White circles in Figure 3 are obtained from numerical analysis for the extreme condition. To get extreme condition, the relaxation times presented by equation (5) and (9) are set to extreme value. Numerical solutions agree with theoretical relations. And this shows that the numerical solutions have good precision.

EXPERIMENT

The authors should mention that they carried out their experiments at inlet temperature and pressure, the experiments are carried out by using the two dimensional convergent-divergent nozzles, which are designed to produce the oblique shock wave near the end of the nozzle.

Two-dimensional convergent-divergent nozzles

The shape of two dimensional nozzles is important to observe the oblique shock waves from the side wall. We prepare two types of those nozzles with and without the inclined wall and try to measure the pressure profiles along the nozzles to compare to each other. The shapes of the two nozzles with and without the inclined wall are drawn on Figure 5. Isentropic Homogeneous Equilibrium (IHE) model is used for the design of the nozzles. The nozzle is cut out from the 0.8-[mm]-thick SUS board with the wire electric discharge machine.

The oblique shock waves are not appeared in the nozzles without the inclined wall, while the pressure at the wall of the nozzle with the inclined wall goes up by the oblique shock waves.

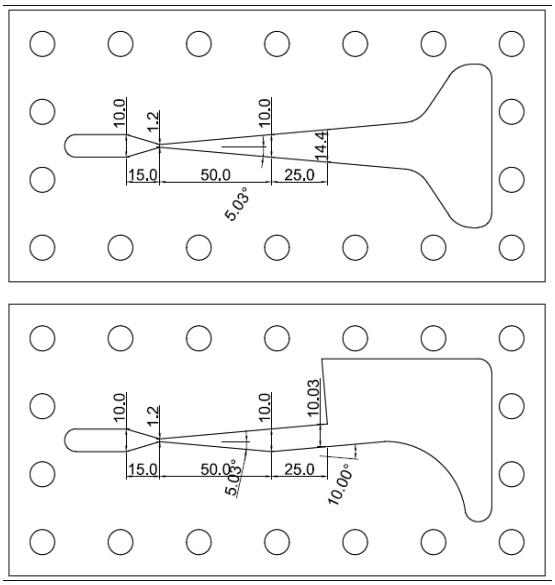

Figure 5 The shape of the two-dimensional nozzles

Measuring method

The chromel-alumel thermocouples are used for a temperature survey, and the pressure gauges are used for pressure measurement on the side wall of two-dimensional convergent-divergent nozzles. The measured temperature is changed into saturation pressure using a steam table. Side wall of the convergent-divergent nozzle plate is made by Bakelite which makes drilling of the small pressure tapes ease. About twenty pressure taps are located along the center line of the nozzle wall and near the divergent nozzle plate (Figure 6).

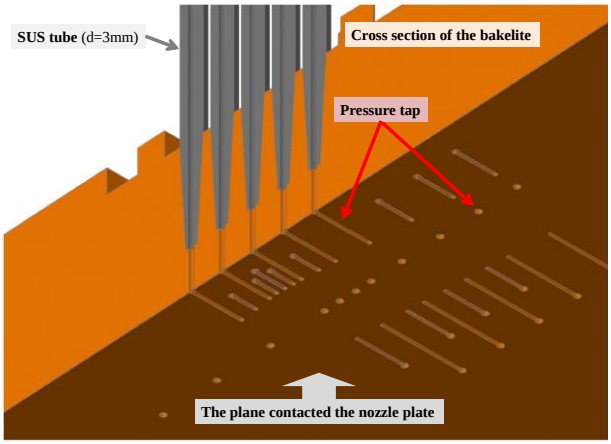

Figure 6 The cross-section view of upper Bakelite

Blow down testing apparatus

Figure 7 shows the feature of the blow down testing apparatus set up for this study. It mainly consists of the high-pressure tank, the test section and the gas cylinders shown in Figure 8. The carbon dioxide blows down from the high-pressure tank, and the high-speed two-phase flow goes through the nozzle in the test section. Nitrogen gas whose density is smaller than that of carbon dioxide is used to compress the high-pressure tank from the top. The flow rate of compressing nitrogen gas is measured by the orifice. Then the volumetric flow rate of the flushing carbon dioxide is calculated from that of nitrogen. The pressure of carbon dioxide at the inlet of the nozzle is controlled by the decompression valve at the high pressure nitrogen cylinder. The temperature of the carbon dioxide is adjusted by the temperature of the hot water which runs through the heat exchanger pipe in the high-pressure tank. The inlet pressure ranges from 9 to 12 [MPa], and the temperature from 10 to 40 [ºC].

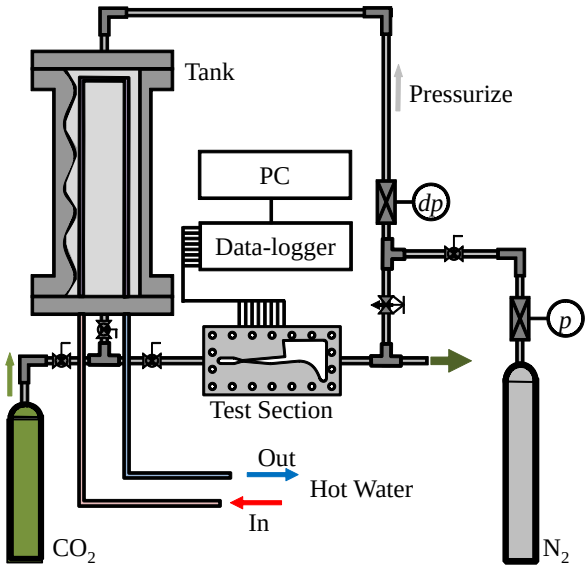

Figure 7 Experimental apparatus

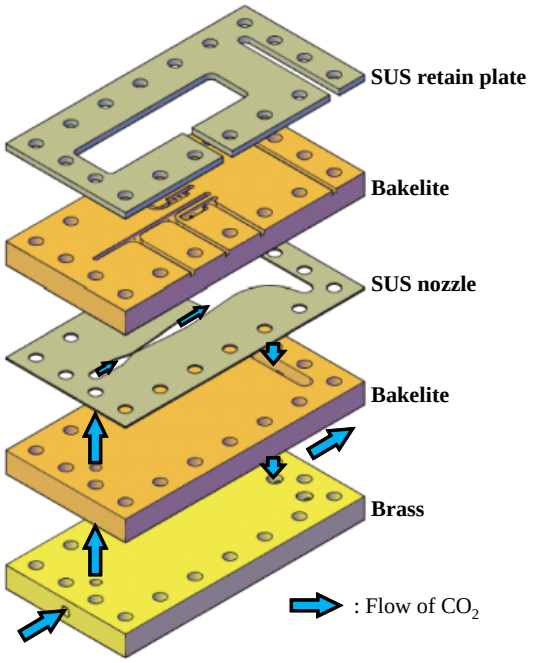

Figure 8 Test section

EXPERIMENTAL RESULT

Pressure profiles in the nozzle

The typical experiment carries out at inlet pressure and temperature conditions of 10.8 [MPa] and 31.2 [ºC]. For this case, the outlet temperature of the nozzle is decreased down to -54.0 [ºC]. The pressure profiles along the nozzle with the inclined wall are shown in Figure 9. The pressure profile plotted by sold line which is calculated from the Isentropic Homogenous flow Model is compared with the measured result. The measured pressure distribution agrees with this theoretical curve. The two-phase flow in the divergent section of the nozzle obviously exhibits the supersonic decompression behavior. The Mach number of two-phase flow predicted by the Isentropic Homogenous flow Model is about 2.17. The pressure increases by the two-phase flow oblique shock waves are detected by the pressure transducer in the nozzle with inclined wall. Both the pressure profiles near wall plates and along the center line of nozzle wall are measured.

Figure 10 shows the precise pressure increase in the nozzle with inclined wall. The pressure profiles near inclined wall plates are plotted by the triangles and those at center line of nozzle wall by the square. The pressure profiles at the wall plate increased earlier than that at the center. This means that the oblique shock waves are appeared in the nozzle. The shock wave angle of the oblique shock wave is determined from this difference and geometrical position of pressure taps.

Comparison with the shock relations on the extreme conditions

Black circle in Figure 3 is the shock wave angle obtained from above mentioned method. The angle of the experimental shock wave is about 66.8 [º]. But the angle of the two-phase flow oblique shock wave predicted by the equilibrium condition is much smaller than this. The angle is rather close to the momentum frozen condition. This means that momentum non-equilibrium processes are occurred in the two-phase flow oblique shock wave and the equivalent Mach number must be considerably small.

Comparison with the numerical solutions

Figure 11 shows comparison of experiments in Figure 9 with numerical analyses. The vertical axis corresponds to the pressure rising by the oblique shock waves instead of absolute pressure in Figure 10. The horizontal axis corresponds to the distance from the start point of inclined wall. Experimental results are plotted by triangles and circles. Formers are the pressures on inclined side wall and latters on opposite side wall. Numerical results are plotted solid lines for the case in which the droplet size is 5 [μm]. After 10 [mm], the experimental pressures are increased because of the reflection of the shock wave. The reflection of wave can be easily understood by the diagram drown in upper side of Figure 10. The pressure increases near the start point are well represented by the numerical analysis. But this analysis cannot explain the reflection of wave. Numerical results with diameter of 2 and 10 [μm] are also plotted by doted and dashed lines. The dotted line is too closer and the dashed line is too far. It is guessed form this experiment that the droplet diameter of the two-phase flow in this nozzle is about 5 [μm].

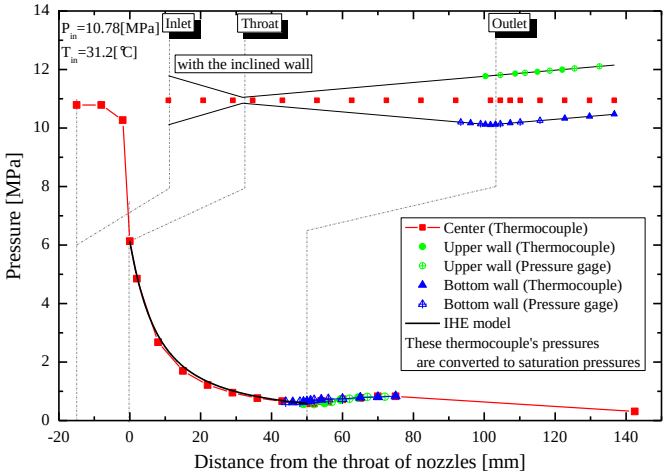

Figure 9 Pressure profiles along the nozzles

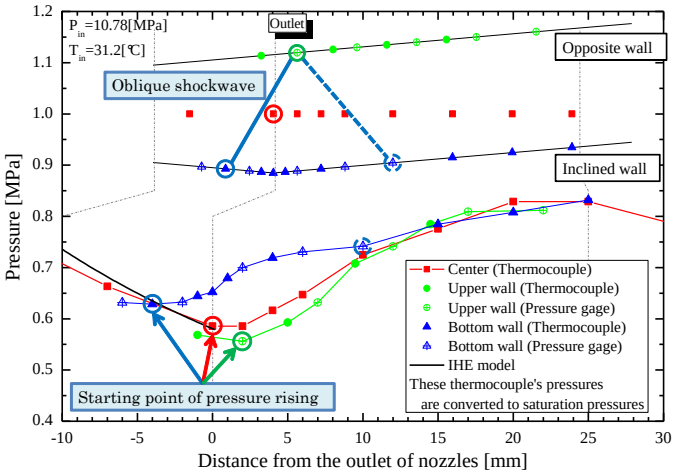

Figure 10 Pressure profiles at the outlet of nozzles

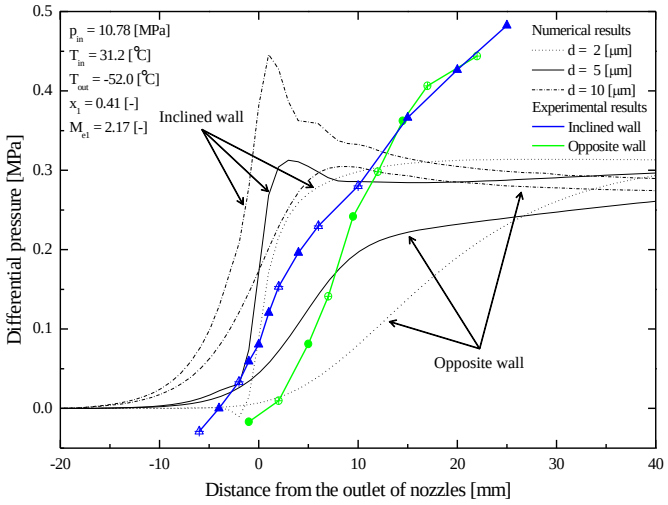

Figure 11 Droplet sizes of experimental results

CONCLUSIONS

Theoretical and experimental study is carried out to elucidate the behaviour of the oblique shock waves in the carbon dioxide two-phase flow. The theoretical oblique shock wave relations are derived for extreme conditions. Numerical analysis is also presented. The oblique shock waves are measured by the experiment using the convergent-divergent nozzle with inclined wall. Numerical results can estimate the experimental results with fairly good precision, but the reflections of the oblique shock wave cannot be predicted. The diameter of the droplet in two-phase flow in the nozzle is guessed to be the order of 5 [μm] and momentum frozen phenomenon occurs in this situation.

REFERENCES

[1] L.D. Landau, E.M. Lifshitz, Fluid Mechanics, *Pergamon Press*, 1959, 422.

[2] Nakagawa, M., Refrigeration Cycle with Two-Phase Ejector, *Refrigeration*, Vol. 79, No. 925, 2004, pp. 856-861.

[3] Nakagawa, M., Takeuchi, H. and Nakajima, K., Performance of Two Phase Ejector in Refrigeration Cycle, *Transactions of the Japan Society of Mechanical Engineers*, Series B, Vol. 64, No. 625, 1998, pp.3060-3067.

[4] Nakagawa, M. and Harada, A., Two-dimensional Rarefaction Waves in the High-speed Two-phase Flow, *Thermal Science and Engineering*, Vol. 15, No. 4, 2007, pp.223-231.

[5] Nakagawa, M., Chino, H. and Harada, A, Two-phase expansion waves at nozzle outlet using CO_2, *Thermal Science & Engineering*. Vol. 16, No. 4, 2008, pp. 139-145.

[6] Harada, A. and Nakagawa, M., Theoretical Analysis of the Two-Phase Oblique Shock Waves in an Ejector with Momentum and Temperature Relaxation, *Transactions of the Japan Society of Refrigerating and Air Conditioning Engineers*, Vol. 27, No. 3, 2010, pp. 13-21.